# Ultrafast Demagnetization Dynamics at the *M* Edges of Magnetic Elements Observed Using a Tabletop High-Harmonic Soft X-Ray Source

Chan La-O-Vorakiat,* Mark Siemens, Margaret M. Murnane, and Henry C. Kapteyn
*Department of Physics and JILA, University of Colorado, Boulder, Colorado 80309-0440, USA*

Stefan Mathias and Martin Aeschlimann
*University of Kaiserslautern and Research Center OPTIMAS, 66606, Kaiserslautern, Germany*

Patrik Grychtol, Roman Adam, and Claus M. Schneider
*Institute of Solid State Research, IFF-9, Research Center Jülich, 52425, Jülich, Germany*

Justin M. Shaw, Hans Nembach, and T. J. Silva
*Electromagnetics Division, National Institute of Standards and Technology, Boulder, Colorado 80305-3328, USA*
(Received 19 May 2009; published 15 December 2009)

We use few-femtosecond soft x-ray pulses from high-harmonic generation to extract element-specific demagnetization dynamics and hysteresis loops of a compound material for the first time. Using a geometry where high-harmonic beams are reflected from a magnetized Permalloy grating, large changes in the reflected intensity of up to 6% at the *M* absorption edges of Fe and Ni are observed when the magnetization is reversed. A short pump pulse is used to destroy the magnetic alignment, which allows us to measure the fastest, elementally specific demagnetization dynamics, with 55 fs time resolution. The use of high harmonics for probing magnetic materials promises to combine nanometer spatial resolution, elemental specificity, and femtosecond-to-attosecond time resolution, making it possible to address important fundamental questions in magnetism.

DOI: 10.1103/PhysRevLett.103.257402 PACS numbers: 78.70.Ck, 75.25.+z, 78.20.Ls

The study of magnetism, magnetic materials, and dynamics in magnetic systems is a topic of fundamental interest in our understanding of correlated systems, as well as being directly relevant to technology and information storage [1]. In recent years, magnetism at ultrafast time scales has been a topic of increasing interest. A thorough understanding of femtosecond magnetism will address the important questions of how fast the magnetization can be reoriented in a material and what physical processes present fundamental limits to this speed. In the spatial domain, magnetism at nanometer length is a topic directly relevant to data storage, since future advances in this technology will require a further reduction in device dimensions to increase the storage density. These considerations have motivated a variety of studies using magneto-optic effects in conjunction with ultrafast light pulses to explore these fundamental limits.

Magneto-optical dynamic studies currently make use either of visible-wavelength light from ultrafast lasers, or x-rays from large-scale synchrotron x-ray facilities. Ultrafast lasers produce short pulses (~30 fs), making possible femtosecond time resolution [2–5], but with a spatial resolution that is generally limited by the wavelength of the probe light. X-rays, on the other hand, allow for high spatial resolution and high contrast imaging at the elemental absorption edges of ferromagnetic materials. However, the available time resolution to date is too slow to resolve the fastest dynamics involved in domain reorientation or to illuminate the physics behind the recently observed ultrafast coherent interactions between light and the electron spin system. Because of this, significant efforts have been devoted to using laser pulses to select a short burst (~100 fs) of x rays from synchrotron radiation (called femtosecond-slicing) [6]. However, these experiments are time consuming and challenging, due to the low flux of sliced photons.

Continued scientific and technological progress thus requires studies that combine nanometer spatial resolution with femtosecond-to-attosecond time resolution. This is a challenging proposition, but one that can be addressed using newly developed tabletop-scale coherent light sources based on high-harmonic up-conversion (HHG) of a femtosecond laser. HHG is an extreme nonlinear process that produces coherent short wavelength beams with the shortest pulse durations demonstrated to date for any light source—in the 0.1 fs to 10 fs range [7–9]. The generated harmonics extend from 10 eV to greater than 2 keV, and retain the polarization and coherence properties of the driving laser under phase-matched generation conditions. Bright HHG beams with sufficient flux for experimental applications can currently be generated with photon energies of up to ~330 eV [9]. Past synchrotron measurements using long duration pulses have shown that the magnetization can be probed at the *M* edges of Fe, Co, and Ni, at photon energies around 55 eV to 65 eV [10–14]. This is an energy range that is easily accessible using HHG.

 

The significance of this work is fourfold. First, the ability to make elementally specific measurements allows us to compare ultrafast demagnetization dynamics in the constituents of a compound material. Second, the ultrafast time resolution of HHG provides a clear pathway for addressing a controversy concerning the time scales and mechanisms associated with the ultrafast (possibly even attosecond) dynamics of magnetization [5,15]. The extremely short pulses provided by HHG can address both electron (<100 fs) and spin dynamics (>300 fs) on an equal footing, which is the prerequisite to studying the mechanisms governing coupling between the electron, spin and lattice subsystems [2]. Recently, Bigot *et al.* [5] investigated coherent ultrafast magnetic phenomena induced by femtosecond laser pulses. This is a new topic for future research in magnetism that requires the ultrahigh femtosecond-to-attosecond time-resolution provided by HHG. Third, the full spatial coherence of the high-harmonic source will enable imaging of magnetic structures with nanometer spatial resolution and ultrafast time resolution. Coherent diffractive imaging has recently been used to acquire images with resolutions of 50 nm using high-harmonic sources in a multiple pulse imaging regime [16], and with a resolution of 120 nm in a single pulse imaging regime [17]. Finally, the high-harmonic source uses a tabletop femtosecond laser that is available in many laboratories worldwide. Therefore, this work represents an accessible new experimental capability for magnetic materials research.

In our experiment, 1.3 mJ, 30 fs pulses from a Ti:sapphire laser amplifier system, operating at a repetition rate of 3 kHz, are coupled into a hollow fused-silica waveguide [Fig. 1(a)]. The waveguide is filled with neon gas within which a broad range of harmonics (from 42 to 72 eV) is phase-matched, spanning both the Fe and Ni $M$ edges. The comb of harmonics emerging from the waveguide is separated from the residual driving laser light using two 200 nm thick aluminum filters. The harmonic beam is focused by glancing incidence reflection from a 2 m focal length gold-coated mirror. Finally, we take advantage of the spatial coherence properties of the high-order harmonics to spectrally resolve the harmonics by diffracting the harmonics from a 1 $\mu$m line (2 $\mu$m period) Permalloy grating [$Ni_{80}Fe_{20}$, Fig. 1(b)]. The beam size incident on the magnetic grating is approximately 500 $\mu$m in diameter. The resulting diffraction pattern is recorded by a windowless CCD. The Permalloy grating was fabricated using photolithography, starting with an ion-beam-deposited thin film consisting of a 3 nm Ti seed layer and a 10 nm Permalloy layer on a thermally oxidized Si wafer. Conventional lift-off processing was used to define a diffraction grating.

A typical harmonic spectrum is displayed in Fig. 2. The HHG process generates odd-order harmonics of the ~780 nm driving laser, resulting in harmonic peaks separated by 3.16 eV. The sharp cutoff in the spectrum (above which no harmonic light is seen) corresponds to the strong

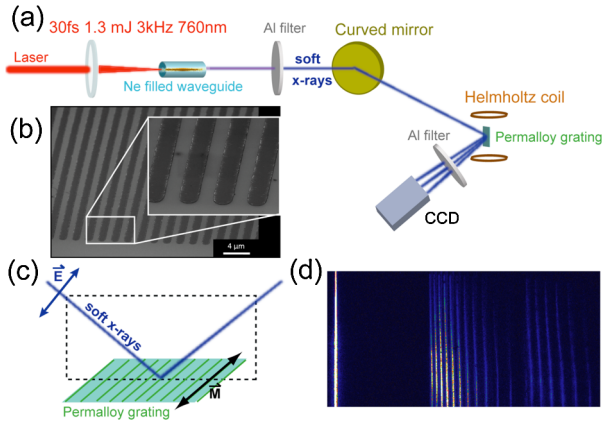


FIG. 1 (color online). (a) Experimental setup. (b) Scanning electron micrograph of the Permalloy grating with a period of 2 $\mu$m. (c) Sample geometry—the blue arrow depicts the $p$-polarized soft x-ray beam whose plane of incidence is shown by the dashed black box. The black arrows indicate the two directions of magnetization reversal, which are perpendicular to the plane of incidence of the probe light. (d) Typical harmonic spectrum reflected from the Permalloy grating and recorded on a CCD.

absorption edge of the aluminum filters at 72 eV. This allows for straightforward calibration of the harmonic spectrum: we identify the photon energy immediately below the Al edge (71.1 eV) and determine the energies of the lower harmonics accordingly.

The experiment is set up in a transverse magneto-optic Kerr effect geometry ($T$-MOKE); i.e., the magnetic field is applied perpendicular to the plane of incidence of the linearly polarized probe light and parallel to the stripe direction of the Permalloy diffraction grating. Unlike

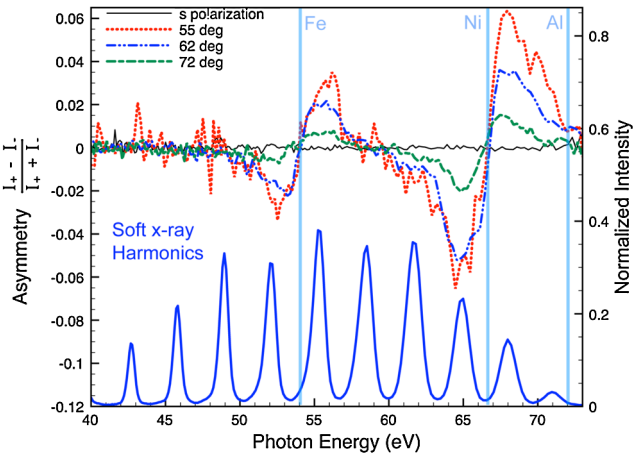


FIG. 2 (color online). Experimental data showing the HHG spectrum (lower plot, right axis) and measured magnetic asymmetry (dashed lines in upper plot, left axis) for different incident angles. No asymmetry is measured for $s$-polarized probe light (black line). The vertical lines denote the Fe, Ni, and Al absorption edges.

MOKE measurements in other geometries, $T$-MOKE induces no ellipticity in a $p$-polarized probe beam. Rather, the reflectivity of the surface changes, depending on the magnetization of the sample [10]. The sample magnetization is oriented by a Helmholtz coil capable of producing 4.8 kA/m (60 Oe) magnetic fields, which exceeds the 0.8 kA/m to 1.6 kA/m (10 to 20 Oe) switching field of the Permalloy grating. The diffracted harmonic intensities are measured at $\pm 4.8$ kA/m ($\pm 60$ Oe).

The strength of the $T$-MOKE signal can be characterized in terms of an asymmetry between two magnetization states, defined as $\mathbf{A} = (I_+ - I_-)/(I_+ + I_-)$ where $I_+$ and $I_-$ denote the reflected intensities recorded for the two magnetization directions. The shape of the resulting asymmetry for different incidence angles of the probe light is shown in the upper plot of Fig. 2 (dashed lines). Large changes in sign and magnitude of asymmetry are observed at the $M$ absorption edges of Ni (68 eV) and Fe (55 eV). The shape of the asymmetry is in agreement both with theoretical arguments based on spin-orbit coupling and exchange splitting of the electronic states involved in the optical transition [12,18], and with the $T$-MOKE measurement from synchrotron radiation [10–13]. We also verified the magnetic contribution on the signal by rotating the plane of polarization of the probed light to $s$-polarized light, where no asymmetry is observed, as shown in Fig. 2. We measured asymmetries of up to 6% near the Ni $M$ edge at an angle of 55° from normal incidence. For angles of incidence further from normal, the measured asymmetry decreases [10].

To demonstrate the utility of large measured magnetic asymmetries for element-specific probing of magnetization, we characterized the magnetic hysteresis of our sample. Figure 3 shows two hysteresis loops, one monitoring the asymmetry close to the Fe edge and the other close to Ni edge. The measurements at both edges yield identical hysteresis loops, with a coercivity of 800 A/m (10 Oe). The observation of nearly identical hysteresis loops for Fe and Ni in Permalloy implies tight exchange coupling of the respective moments, as was previously inferred from time-resolved x-ray magnetic circular dichroism (XMCD) measurements of Permalloy films by Guan *et al.* [19].

Soft x-ray light at energies above the absorption edge has a short penetration depth of only a few tens of nanometers in most materials. This effect can be exploited to probe the surface properties or near-surface layers of a magnetic structure. In order to demonstrate this ability, we measured the $T$-MOKE asymmetry for Permalloy gratings with palladium (Pd) capping layers of different thickness (2 nm to 15 nm), sputtered on top of the Permalloy gratings. Pd was used because it does not oxidize or have an absorption edge near either the Ni or Fe edges. This allows us to measure the decay of the $T$-MOKE asymmetry due to absorption of the soft x-ray light by the Pd overlayer. Tabulated data for Pd, with an assumed density of $1.2 \times 10^4$ kg/m$^3$, predict attenuation lengths of 3.6 and 3.3 nm, at 55 and 67 eV, respectively, for our angle of incidence around 65° [21]. Figure 4 displays the $T$-MOKE asymmetry near the Ni and Fe absorption edges, which decays exponentially as a function of capping layer thickness. Fits to the data yield decay lengths of $3.02 \pm 0.4$ nm (Ni edge) and $2.68 \pm 0.9$ nm (Fe edge). We assume the discrepancy with tabulated data is probably the result of the reduced density for such ultrathin sputtered films. Nevertheless, this data shows the potential for using $M$ edge $T$-MOKE as a near-surface-sensitive magnetic probe.

Finally, we demonstrate the use of few-femtosecond high-harmonic beams to probe the dynamics of ultrafast demagnetization processes after excitation by an intense infrared pump pulse. Initially, the ultrafast intense pump pulse coherently interacts with the electron and spin systems within the duration of the laser pulse [5]. Then,

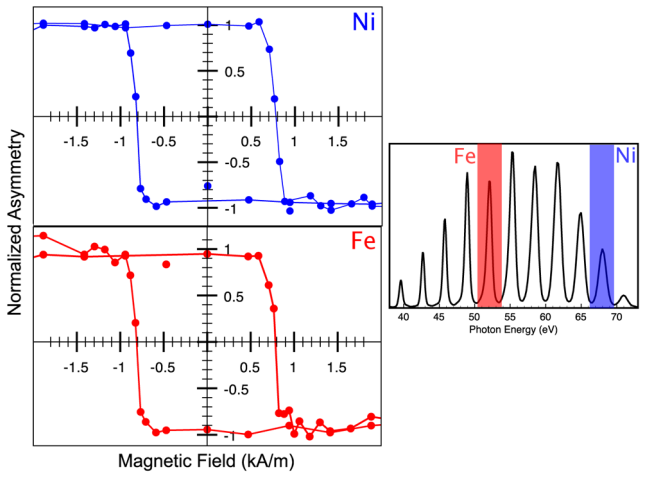


FIG. 3 (color online). Hysteresis loop of the magnetic asymmetry measured near the Ni (top) and Fe (bottom) $M$ edges, with the selected energies indicated on the right.

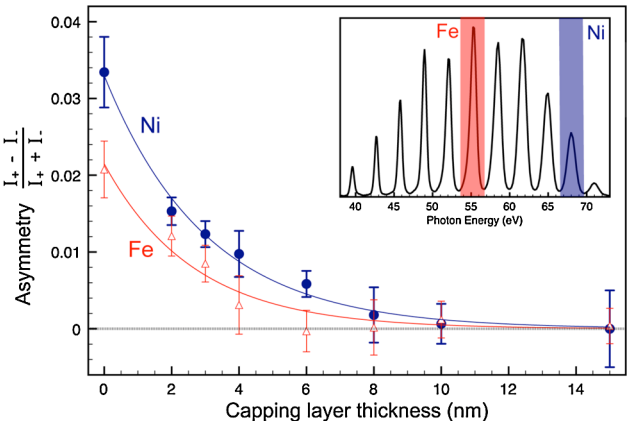


FIG. 4 (color online). Demonstration of the near-surface sensitivity of $T$-MOKE using high-harmonic beams. The measured asymmetry near the Fe (circle) and Ni (triangle) edges is plotted as a function of Pd capping layer thickness. The curves correspond to an exponential decay length of ~3 nm in each case.

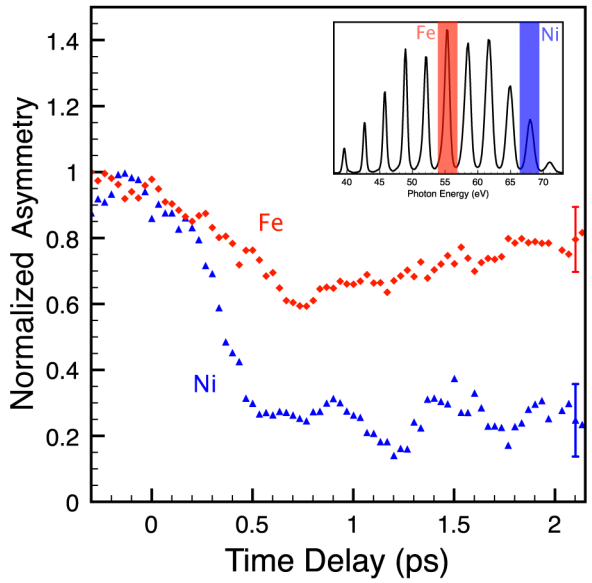


FIG. 5 (color online). Ultrafast, element-selective measurement of demagnetization following laser-pulse excitation of both Ni and Fe components of Permalloy. The magnetic orientation decreases for Fe and Ni on similar time scales of 400 fs. For this measurement, the time resolution is 55 fs. Error bars of the measurements are represented at the 2.1 ps data points.

thermalization of the electron and spin systems takes place through incoherent scattering processes, resulting in a subsequent reduction and reorientation of the magnetization vectors [2–5].

To demagnetize the sample, a pump beam (which was derived from a portion of the HHG generating beam) is incident on the sample with a fluence of 1 $mJ/cm^2$. We choose harmonics around Fe (55 eV) and Ni (68 eV) $M$ edges to measure the asymmetry as a function of time-delay after the pump pulse. Figure 5 shows a reduction in the asymmetry parameter within ~400 fs after excitation of the surface by the pump beam, in agreement with past measurements using visible light [4]. We do not see a significant difference in the demagnetization dynamics curves for Fe and Ni even during the nonadiabatic heating process (within the experimental error of the data), because of the strongly exchange coupled Permalloy system. The time resolution in our experiment is about 55 fs, and limited by the pump-probe geometry [21] and the duration of the pump beam (30 fs). In the future, by using a collinear pump-probe geometry it should be possible to investigate coherent magnetization dynamics [5] on few-femtosecond-to-attosecond time scales [22].

In summary, we have demonstrated the use of ultrafast, coherent, high-harmonic beams to probe magnetization dynamics with elemental specificity, and achieve the fastest time resolution measured to date using any source. The strong signals obtained using HHG as a probe allows for element-specific measurements of ultrafast magnetization processes. High magnetic signal asymmetries of 4% and 6% were measured near the $M$ edges of Fe (55 eV) and Ni (68 eV), respectively. This work opens up the possibility of probing magnetic dynamics and image domain structure on ultrafast femtosecond-to-attosecond time scales, with nanometer resolution, near-surface sensitivity, and element specificity. Finally, recent advances in generating bright, high-harmonic x-ray beams at higher photon energies should enable magnetic material studies at the $L$ absorption edges [9,23] and using circular polarized light [24] in the near future.

The authors gratefully acknowledge funding from the U.S. Department of Energy and the NSSEFF program. This research used facilities provided by the NSF Engineering Research Center in EUV Science and Technology. Contribution of the National Institute of Standards and Technology, an agency of the U.S. government, not subject to U.S. copyright. We also acknowledge useful discussions with D. Steil and M. Cinchetti.

*Chan.La-o-vorakiat@colorado.edu

[1] I. Žutić, J. Fabian, and S. Das Sarma, Rev. Mod. Phys. **76**, 323 (2004).
[2] E. Beaurepaire *et al.*, Phys. Rev. Lett. **76**, 4250 (1996).
[3] M. Cinchetti *et al.*, Phys. Rev. Lett. **97**, 177201 (2006).
[4] I. Radu *et al.*, Phys. Rev. Lett. **102**, 117201 (2009).
[5] J. Bigot, M. Vomir, and E. Beaurepaire, Nature Phys. **5**, 515 (2009).
[6] C. Stamm *et al.*, Nature Mater. **6**, 740 (2007).
[7] H. C. Kapteyn, M. M. Murnane, and I. R. Christov, Phys. Today **58**, No. 3, 39 (2005).
[8] A. Rundquist *et al.*, Science **280**, 1412 (1998).
[9] T. Popmintchev *et al.*, Proc. Natl. Acad. Sci. U.S.A. **106**, 10 516 (2009).
[10] H. Höchst *et al.*, J. Appl. Phys. **81**, 7584 (1997).
[11] M. Pretorius *et al.*, Phys. Rev. B **55**, 14133 (1997).
[12] M. Sacchi *et al.*, Phys. Rev. B **58**, 3750 (1998).
[13] M. Hecker *et al.*, J. Electron Spectrosc. Relat. Phenom. **144–147**, 881 (2005).
[14] S. Valencia *et al.*, New J. Phys. **8**, 254 (2006).
[15] G. P. Zhang *et al.*, Nature Phys. **5**, 499 (2009).
[16] R. Sandberg *et al.*, Opt. Lett. **34**, 1618 (2009).
[17] A. Ravasio *et al.*, Phys. Rev. Lett. **103**, 028104 (2009).
[18] J. L. Eskine and E. A. Stern, Phys. Rev. B **8**, 1239 (1973).
[19] Y. Guan *et al.*, J. Magn. Magn. Mater. **312**, 374 (2007).
[20] CXRO X-Ray Interactions with Matter website http://henke.lbl.gov/optical_constants/.
[21] The probe beam with the diameter ($x$) of approximately 0.5 mm overlaps with the pump at a relative angle $\theta = 1.5°$, introducing a time smear of $t_{res} \approx x \sin\theta/c$ where $c$ is the speed of light.
[22] I. Thomann *et al.*, Opt. Express **17**, 4611 (2009).
[23] T. Popmintchev *et al.*, Opt. Lett. **33**, 2128 (2008).
[24] X. Zhou *et al.*, Phys. Rev. Lett. **102**, 073902 (2009).